CONVOLUTIONAL SVM NETWORKS FOR DETECTION OF *GANODERMA BONINENSE* AT EARLY STAGE IN OIL PALM USING UAV AND MULTISPECTRAL PLEIADES IMAGES

P. Ahmadi [1]*, S. B. Mansor [2], H. Ahmadzadeh Araji [3], B. Lu [4]

[1]Department of Geography, Simon Fraser University, 8888 University Drive, Burnaby, BC V5A 1S6, Canada - parisa_ahmadi@sfu.ca

[2]Geospatial Information Science Research Centre, Faculty of Engineering, Universiti Putra Malaysia, 43400 Serdang, Selangor, Malaysia - shattri@eng.upm.edu.my

[3]Texas A&M AgriLife Research & Extension Center, 1509 Aggie Drive, Beaumont, TX 77713, USA - hamidreza.araji@aesrg.tamu.edu

[4]Department of Geography, Simon Fraser University, 8888 University Drive, Burnaby, BC V5A 1S6, Canada - b_lu @sfu.ca

Commission IV, WG IV/3

KEY WORDS: Basal stem rot, Support Vector Machine, UAV, Pleiades.

ABSTRACT:

Oil palm performs a considerable role in Malaysia's economic system as Malaysia is the second-biggest palm oil manufacturer in the world. In oil palm plantations. Basal stem rot (BSR) is a disease caused by *Ganoderma boninense* that is responsible for a considerable annual losses, particularly in South East Asia. The disease remains an unresolved problem in most production areas due to lack of disease management strategy to detect the infected palms at their early stage. In recent years, advancement in remote sensing platforms and image processing methods have produced remarkable results for the detection of diseases at early stage. In this study, support vector machine (SVM) classifier was performed on UAV and Pleiades imagery to determine the ideal classification model for the early diagnosis of BSR disease in oil palms. The investigation's results showed that UAV provided the most accurate prediction, with a total accuracy of 68.28%, while 64.52% of the early Ganoderma infections could be identified with accuracy levels of 64.07% and 64.49%, respectively. The early Ganoderma infection could be recognized with an overall accuracy of 64.07% and 64.49%, respectively, while the Pleiades had an overall accuracy of 68.28% and 64.52%. Although the categorization accuracy appeared to be only modest at first glance, the quantity of detail offered by the imageries suggested that the accuracies were acceptable.

1 INTRODUCTION

Recent devastating *Ganoderma boninense* attacks on oil palm due to basal stem rot (BSR) in Southeast Asia have caused significant post-harvest losses; about RM225 million to RM1.5 billion a year (Ommelna et al. 2012). The economic loss caused by this pathogen could be severe and cause impacts on the strategic and scientific management of oil palm plantations. The devastation, however, has stirred a lot of interest among researchers to work on the possibility of a remote sensing approach method to identify *Ganoderma* infected palms that will help to mitigate any damage in the future. The detection and differentiation of the disease at its earliest stage of infection can extend the productive life of the infected oil palm (Hillnhuetter and Mahlein, 2008. Nevertheless, it is costly and time-consuming to visually monitor this disease in the field during its early phases. (Liaghat et al. 2014; Zamry et al. 2015). In the early stage of *Ganoderma* infection, palms are symptomless making it difficult to diagnose.. Hence, alternative evaluations are required. Researchers have experimented with numerous remote sensing platforms in discriminating between healthy and diseased plants (Ahmadi et al. 2016; Lelong, 2010; Shafri et al. 2012;), and they have investigated various classification algorithms for differentiation of disease levels (Al-hiary et al. 2011; Patil and Kumar, 2011). Additionally, remote sensing methods could also be developed to distinguish BSR infections on both small- and large-scales within oil palm plantation areas. Ahmadi et al. (2016) analysed leaf spectral data obtained from the GER spectroradiometer with artificial neural network (ANN) for detection of Ganoderma infected oil palms at early stage. The results provided through the ANN analysis on healthy and early stage Ganoderma infected oil palms illustrated satisfactory classification with an accuracy of 83.3% and 100.0% in the 540-550 nm spectral region, respectively. In BSR related research, while the use of Unmanned Aerial Vehicles (UAV) is still considerably limited, they may play a key role in improving detection of infected oil palms, especially at their early stage. Several limitations associated with satellite data, including low spatial resolution, cloud spots, and long revisiting times in relatively small geographical areas have been avoided by the use of UAVs; however, UAVs are not suitable for large-scale applications due to time and cost limitations (Fornace et al. 2014). Due to the spectral reflectance difference in plants that is well associated with various degrees and types of stress, digital (red, green, and blue), multispectral, hyperspectral, fluorescence imaging, and thermal infrared-based optical sensors have recently become widely used in assisting plant disease detection (West et al. 2003; Liu et al. 2007; Naidu et al. 2009; Yang et al. 2009; Balasundaram et al. 2009; Zhang et al. 2012; Tawfik et al. 2013; Alexander et al. 2014; Dayou et al. 2014). based on the fact that infected plant has different spectral reflectance compared to healthy plants and exhibit significantly higher spectral reflectance in the visible range (400–700 nm), also due to changes in physiology and biochemistry in the leaves fallowed by stress (Govender et al. 2009; Sanches et al. 2014). while healthy plants show lower spectral patterns Govender et al. 2009; Sanches et al. 2014). By analyzing digital images, new classification approaches like ANN and SVM have been widely used to assist farmers and producers identify early symptoms of plant diseases (Pourreza et al. 2016; Calderon et al. 2015; Patil

and Zambre, 2014; Rumpf et al. 2010; Camargo and Smith, 2009). a sophisticated plant disease detection method using machine learning classifiers can quickly, accurately, and dependably identify plant diseases in their early stages for economic, production, and agricultural benefits (Sankaran et al. 2010). In plant disease identification study, artificial selection of SVM parameters in the classification of the samples is usually relied upon. The function class for the classification model can be arbitrary complex as a result of learning with SVMs, giving it the flexibility for challenging classification tasks. Capabilities of SVM for advanced disease detection have been proven through many studies. Pourreza et al. (2016), for instance, described how to use an SVM model for differentiable wavelengths to identify Citrus Black Spot (CBS), a fungal disease that affects citrus species, with overall accuracy rates of 94.6%. In a different investigation, Calderon et al. (2015) looked at the potential of linear discriminant analysis (LDA) and SVM classifier on high-resolution thermal and hyperspectral imagery for detection of Verticillium wilt (VW) infection in many stages in olive. Their findings depicted that, despite the LDA classifying trees more accurately in their early stages of infection, SVM had a higher total accuracy (79.2% vs. 59.0%). Given this information, no prior research have connected the physiological changes in diseased oil palms at the canopy level that can be detected through imagery. Therefore, the objective of this study was to discriminate BSR disease levels derived from UAV and Pleiades images using the SVM model.

2 MATERIAL AND METHODS

Study Area

The study was carried out on a United Malacca Berhad oil palm field in the Machap sub-district of Melaka, Malaysia (2.402° N 102.327° E), which was formerly a rubber plantation. Study subjects were 12 years old mature oil palm trees that were planted in 2002 Based on particular visual symptoms on the canopy and the presence of basidiocarps on the basal of the palms, we recognized and designated 374 assessed palms in the field with four stages of infection during field data collecting in October 2014. Trunk samples were obtained by trunk drilling in order to perform a GSM test on palms lacking a Ganoderma fruiting body in order to confirm the existence of a fungus related to Ganoderma. The samples were divided into four categories labeled as T1 (healthy), T2 (mildly infected), T3 (moderately infected), and T4 (supported by both visual symptoms and GSM check results) (severely infected). With the use of a global positioning system (GPS) receiver and a palm triangulation map, the palms were later individually geolocated in the UAV image.

Multispectral Camera

The acquired composite infrared (CIR) UAV image of the selected site was obtained on 31 October 2014, has 3 spectral bands of red, green, and infrared (NIR,) and the spatial resolution of imagery is 0.026 m/pix (Figure 1). It has covered up to 0.089 km^2 and flown at an altitude of 91.3 m above ground level. In this study, a hexacopter UAV system was deployed, and we got 107 photos that were mosaicked using the Agisoft® PhotoScan program (Agisoft LLC, St. Petersburg, Russia). Later, the SVM classification was performed using digital number values (García- Ruiz et al. 2013).

On September 16, 2016, 0.5 m (panchromatic mode) and 2 m (multispectral mode) resolution Pleiades satellite images were collected (Figure 1). The Pleiades sensor has 4 spectral bands (b0, 0.43–0.55 μm; b1, 0.50–0.62 μm; b2, 0.59–0.71 μm; b3, 0.74–0.94μm). The image was geometrically corrected, and coordinates of surveyed trees were overlaid Pleiades image whereby a region of interest was selected for the model input. The satellite image was free from cloud covers and the classification was performed using digital number values (Trisakti, 2017). The imaging camera was calibrated and corrected before image acquisition using a variety of methods, including flat field from look-up tables (LUT) correction, and Brown-Conrady model techniques for lens distortion corrections (Wang et al. 2009; Hugemann et al. 2010) for lens distortion corrections; vignetting correction, where the image data were corrected through a per-pixel multiplication (Goldman et al. 2010; Kim et al. 2008) and radiometric calibration based on empirical line regression models, where a tarpaulin with various colours on it was used for environmental Lambertian reflectance, also known as a pseudo- invariant (PIFs) (Moran et al. 2001; Karpouzli et al. 2003).

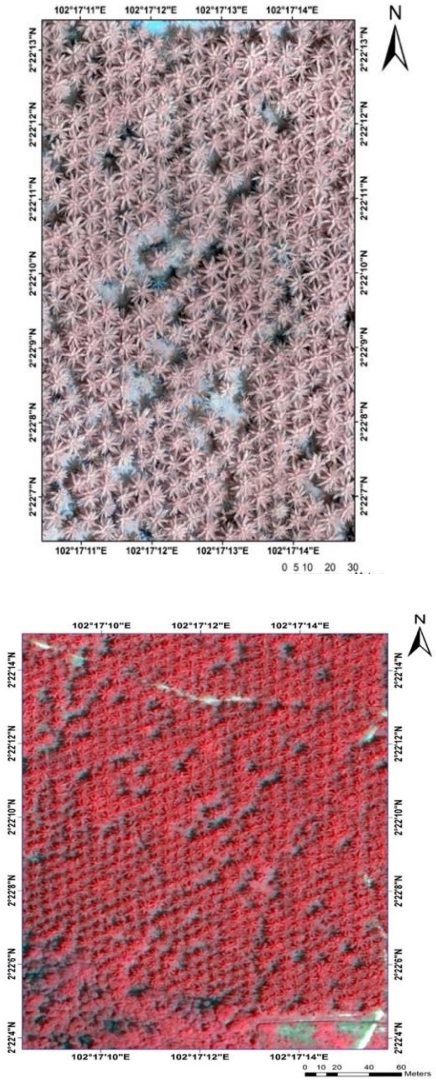

Figure 1. The UAV CIR image of the study area (top) and the Pleiades image (bottom).

SVM Classification

Support vector machine is a nonlinear classifier that constructs a model that categorizes fresh instances into either one category or the other, making it a non-probabilistic binary linear classifier. The SVM model includes a supervised learning classification A

supervised learning classification technique based on the idea of decision planes that specify decision boundaries is included in the SVM model. A decision plane is a structure that divides a collection of objects with various class memberships. All SVM algorithms were implemented with MATLAB 2014. The implementation of multi- classes SVM was used for the classification of distinct levels of *Ganoderma* infected palms. The SVM algorithms for the UAV and Pleiades images were designed to execute two main procedures: space extraction and classification. The first phase was feature extraction, consisting of spectral and structural features extraction. Red (R), green (G), blue (B), near-infrared (NIR), digital numbers (DNs), and a vegetation index namely Normalized Difference Vegetation Index (NDVI) provides an indication of vegetation health and a way to track changes in vegetation were the descriptors used to describe the spectral properties. The selected structural features were average, variance, and grey-level co-occurrence matrix (GLCM). Average, variance, and a matrix of the co-occurrence of grey levels (GLCM) were the structural features that were chosen. The spatial relationship between pixels is taken into account by the GLCM, a statistical technique for analyzing texture (grey-level co-occurrence matrix, also known as the grey-level spatial dependence matrix). The GLCM functions characterize the texture of an image by calculating how often pairs of the pixel with specific values and in a specified spatial relationship occur in an image, creating a GLCM, and then extracting statistical measures from this matrix. The GLCM is better than texture filter functions since the latter cannot provide information about the spatial relationships of pixels in an image. The SVM classifier was used in the second phase to produce the most accurate classification by integrating training and test data with specific features. Finally, the outputs of models were coloured onto classified images based on the training data. It is worth to mention that the aim of this study was to detect early the *Ganoderma* infection, and therefore we focused on classifying T1, T2, and T3, and excluded T4 because the latter could be easily visually detected through human sights.

3 RESULTS AND DISCUSSION

Figure 2 presents the SVM classified map generated from the UAV image. The regions that were classified as unknown belonged to soil surface, shrub, rotten trees, or the trees that were not in the main classes. According to Table 1, the accuracy of various classes had different trends, such that the highest producer accuracy belongs to T1, then T3, and finally T2. Since producer accuracy indicates the quality of classification, it could be concluded that for classification of UAV image using the SVM, the model precision for the T1 class was appropriate (88.4%), but the model was not capable of classifying mildly infected (T2) pixels as well as those of T1. It is important to note that the largest number of unknown pixels was related to the T2 class and that by neglecting these pixels, the accuracy of this class could rise to 79.4%. The result for healthy trees could be considered appropriate since among all the T1 pixels, only a few were misclassified in T2 and none of them was detected as moderately infected. On average, the SVM accuracy for UAV imaging was 68.28% and a kappa coefficient of 0.57.

The classified Pleiades image is depicted in Figure 3 and Table 2 summarizes the results of Pleiades image classification using the SVM algorithm on three different severity classes. As the disease progressed, the classifier accuracy diminished, such that the lowest user produced accuracy acquired for moderately infected palms (T3). A high number of unknown and T3 pixels was misclassified as T1, contributing to its low accuracy. However, since the aim of the study was the detection of *Ganoderma* at its early stage, we focused on the T2 class. By neglecting the unknown pixels in this class, a higher percentage of true classified pixels, which was 76.78%, appeared. Nevertheless, the SVM classifier was neither able to detect them nor categorize them as unknown, leading to a relatively low overall accuracy of classification. The overall classification accuracy was more than 64.5%, with a kappa coefficient of 52%. Comparing to the UAV classification areas, the Pleiades image resulted in 1.25 ha of T1, 0.72 ha of T2 and 0.74 ha of T3 versus 1.32 ha of T1, 0.72 ha of T2 and 0.82 ha of T3. Generally, the area classified from both images was similar for the T2, yet was slightly higher for T1 and slightly lower for T3 for the UAV image.

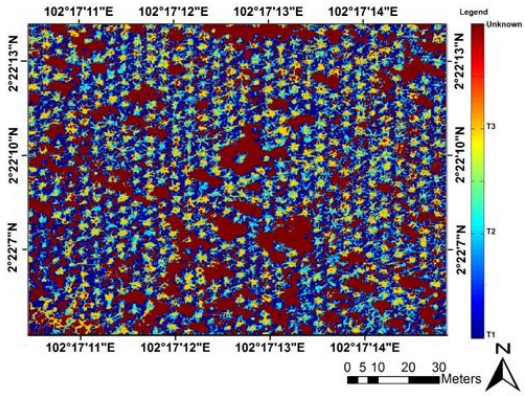

Figure 2. The UAV-SVM classified map.

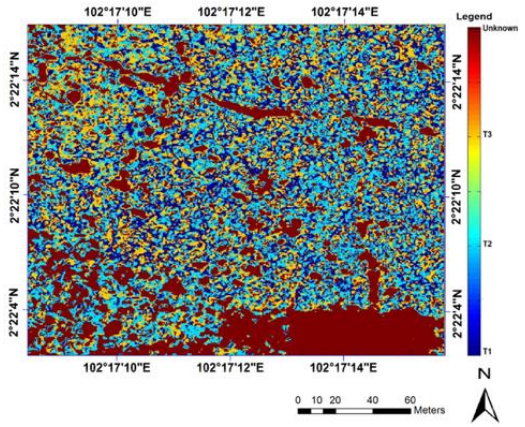

Figure 3. The Pleiades SVM classified map.

	T1	T2	T3	Unknown	Producer Accuracy (Precision)
T1	1065	50	0	90	88.38%
T2	98	2030	430	610	64.07%
T3	74	490	1800	265	68.47%
Unknown	150	30	843	1845	
Truth overall	1387	2600	3073	2810	
User Accuracy (Recall)	76.78%	78.07%	58.57%		68.28% K = 0.57

Table 1. Confusion matrix of SVM classification for UAV imagery.

	T1	T2	T3	Unknown	Producer Accuracy (Precision)
T1	1559	76	587	300	83.54%
T2	0	1173	60	171	64.49%
T3	590	35	2098	530	61.82%
Unknown	934	245	0	1585	
Truth overall	1529	2745	3083	2586	
User Accuracy (Recall)	76.72%	76.43%	50.57%		64.52% K = 0.52

Table 2. Confusion matrix of SVM classification for Pleiades imagery.

4 CONCLUSUION

Generally, the classification accuracy of individual severity classes diminished with severity levels. All in all, the best classification result was achieved for the healthy palms and then for those with slightly infected severity, possibly due to distinct reflectance characteristics of T1 group collected from many palm samples in comparison to the T2 and T3 groups. Due to the nature of the disease distribution that is almost impossible to have a balanced number of infected palms in each class, we acquired fewer samples for the T2 and T3, and that might be attributed to the poor training process of the SVM algorithm. Another reasonable hypothesis is that the spectral reflectance of early Ganoderma infected palms might not be as clear as healthy or moderately infected palms of which the symptoms of the disease have already appeared on the palms, and hence the presence of many ambiguous areas could affect the misclassification between these two classes. The highest false classification in each class at both images was related to unknown pixels that were mixed pixels comprised of soil surface and shrubs. These mixed pixels, consequently, resulted in spectral reflectance that was not unique to any classes. Presence of the mixed pixels could contribute to high misclassification rates since the model was not able to provide clear classification separations between the classes. Although the UAV image had a better accuracy for the classification of unknown pixels due to higher spatial resolution, in both images tested, the highest number of false classifications in T2 category belonged to these unknown pixels. The SVM method, in fact, proved to be a more effective alternative to create an algorithm for early diagnosis of Ganoderma by avoiding these uncertain areas. Nonetheless, these results are in accord with the recent study by Santoso et al. (2010) who demonstrated that the accuracy of BSR detection using Quickbird imagery was about 62% and 67% only. It is worth noting that these imageries which obtained the images of the palms at their canopy level, might have lost vital information related to the biochemical properties of the palms infected by the disease such as affected chlorophyll content (Shafri and Hamdan, 2009), in comparison to the measurements acquired at the leaf level that was via the spectroradiometer. Hence it is reasonable to justify the misclassification occurred through ambiguous characteristics of reflectance observed from the disease since they could be confounded by secondary factors such as leaf area index, leaf arrangement and within canopy shadow (Guyot et al. 1989). The results also indicated that the classification accuracy of Ganoderma infected trees obtained from the UAV was slightly higher than the Pleiades image. This could be attributed by the very high spatial resolution of the UAV image whereas the use of Pleiades image for early-stage detection was limited by the spatial resolution that was insufficient to detect individual palm canopies or infestation. In addition, variability in the experimental conditions, of which the images were taken at different dates, could be also a contributing factor.

The use of SVM algorithms in our study demonstrated the potential of utilizing the data mining approach to facilitate the monitoring of Ganoderma disease at its early stage. The performance of the SVM algorithm was superior in classifying plant diseases at their early-stage infections, such as demonstrated by (Rumph et al. 2010) but not in our study. This could be subject to the use of a ground based spectroradiometer whereby the purity of the signal related to the diseases might not be compromised as much as in the UAV and satellite images that we tested. At the aircraft level, Calderon et al. (2015) found that micro-hyperspectral images from 260 bands analysed with SVM correctly classified asymptomatic olive trees with up to 99.4% accuracy, although trees at their initial and low stage infection were poorly classified, with an accuracy of 14.3% and 40.6%, respectively. In this study, our UAV images were acquired from a modified CIR camera that only has 3 bands yet achieved 64.07% discrimination accuracy. To the best of our knowledge, no evaluation of the images from the aforementioned remote sensing platforms for Ganoderma detection has been reported or published so far. The SVM is potentially one of the machine learning algorithms that could be used for detection of disease at an early stage, yet further improvement is necessary to improve the classifier's performance.

ACKNOWLEDGEMENTS

We would like to thank United Malacca Berhad for the financial support and providing the study area to conduct this study.

REFERENCES

Ahmadi, P., Muharam, F.M., Ahmad, K., Mansor, S., Abu Seman, I., 2017. Early detection of Ganoderma basal stem rot of oil palms using artificial neural network spectral analysis. Plant disease, 101(6), pp.1009-1016.

Al-Hiary, H., Bani-Ahmad, S., Reyalat, M., Braik, M., ALRahamneh, Z., 2011. Fast and accurate detection and classification of plant diseases. Machine learning, 14(5).

Arivazhagan, S., Shebiah, R.N., Ananthi, S., Varthini, S.V., 2013. Detection of unhealthy region of plant leaves and classification of plant leaf diseases using texture features. Agricultural Engineering International: CIGR Journal, 15(1), pp.211-217.

Balasundaram, D., Burks, T. F., Bulanon, D. M., Schubert, T., Lee, W. S. 2009. Spectral reflectance characteristics of citrus canker and other peel conditions of grapefruit. Postharvest Biol. Technol. 51:220-226.

Bauriegel, E., Giebel, A., Geyer, M., Schmidt, U., Herppich,W. B. 2011. Early detection of Fusarium infection in wheat using hyperspectral imaging. Comput.Electron. Agric. 75:304-312.

Brudzewski, K., Osowski, S., Markiewicz, T., 2004. Classification of milk by means of an electronic nose and SVM neural network. Sensors and Actuators B: Chemical, 98(2-3), pp.291-298.

Calderón, R., Navas-Cortés, J.A., Zarco-Tejada, P.J., 2015. Early detection and quantification of Verticillium wilt in olive using hyperspectral and thermal imagery over large areas. Remote Sensing, 7(5), pp.5584-5610.

Camargo, A., Smith, J.S., 2009. Image pattern classification for the identification of disease-causing agents in plants. Computers and Electronics in Agriculture, 66(2), pp.121-125.

Dayou, J., Alexander, A., Sipaut, C. S., Phin, C. K., Chin, L. P. 2014. On the possibility of using FTIR for detection of Ganoderma boninense in infected oil palm tree. IJAAEE 1:161-163.

De Castro, A.I., Ehsani, R., Ploetz, R., Crane, J.H., Abdulridha, J., 2015. Optimum spectral and geometric parameters for early detection of laurel wilt disease in avocado. Remote Sensing of Environment, 171, pp.33-44.

Fornace, K.M., Drakeley, C.J., William, T., Espino, F., Cox, J., 2014. Mapping infectious disease landscapes: unmanned aerial vehicles and epidemiology. Trends in parasitology, 30(11), pp.514-519.

Garcia-Ruiz, F., Sankaran, S., Maja, J.M., Lee, W.S., Rasmussen, J., Ehsani, R., 2013. Comparison of two aerial imaging platforms for identification of Huanglongbing-infected citrus trees. Computers and Electronics in Agriculture, 91, pp.106-115.

Glezakos, T.J., Moschopoulou, G., Tsiligiridis, T.A., Kintzios, S. , Yialouris, C.P., 2010. Plant virus identification based on neural networks with evolutionary preprocessing. Computers and electronics in agriculture, 70(2), pp.263-275.

Govender, M., Dye, P. J., Weiersbye, I. M., Witkowski, E. T. F., Ahmed, F. 2009. Review of commonly used remote sensing and ground-based technologies to measure plant water stress. Water S.A. 35:741-752.

Guyot, G., Guyon, D., Riom, J., 1989. Factors affecting the spectral response of forest canopies: a review. Geocarto International, 4(3), pp.3-18.

Harini, D. N. D., Bhaskari, D. L. 2011. Identification of leaf diseases in tomato plant based on wavelets and PCA. Pages 1398-1403 in: World Congress on Information and Communication Technologies.

Hillnhuetter, C., Mahlein, A.K., 2008. Early detection and localisation of sugar beet diseases: new approaches. Gesunde Pflanzen, 60(4), pp.143-149.

Karimi, Y., Prasher, S. O., Patel, R. M., Kim, S. H. 2006. Application of support vector machine technology for weed and nitrogen stress detection in corn. Comput. Electron. Agric. 51:99-109.

Liaghat, S., Ehsani, R., Mansor, S., Shafri, H.Z., Meon, S., Sankaran, S. and Azam, S.H., 2014. Early detection of basal stem rot disease (Ganoderma) in oil palms based on hyperspectral reflectance data using pattern recognition algorithms. International journal of remote sensing, 35(10), pp.3427-3439.

Liu, Z.Y., Huang, J.F., Shi, J.J., Tao, R.X., Zhou, W., Zhang, L.L., 2007. Characterizing and estimating rice brown spot disease severity using stepwise regression, principal component regression and partial least-square regression. Journal of Zhejiang University Science B, 8(10), pp.738-744.

Naidu, R. A., Perry, E. M., Pierce, F. J., Mekuria, T. 2009. The potential of spectral reflectance technique for the detection of grapevine leaf rollassociated virus-3 in two red-berried wine grape cultivars. Comput. Electron. Agric. 66:38-45.

Noh, H., Zhang, Q., Shin, B., Han, S., Feng, L. 2006. A neural network model of maize crop nitrogen stress assessment for a multi-spectral imaging sensor. Biosyst. Eng. 94:477-485.

Ommelna, B.G., Jennifer, A.N., Chong, K.P., 2012. The potential of chitosan in suppressing Ganoderma boninense infection in oil-palm seedlings. J Sustain Sci Manage, 7(2), pp.186-192.

Patil, J.K., Kumar, R., 2011. Advances in image processing for detection of plant diseases. Journal of Advanced Bioinformatics Applications and Research, 2(2), pp.135-141.

Patil, S.P., Zambre, R.S., 2014. Classification of cotton leaf spot disease using support vector machine. International Journal of Engineering Research and Applications, 4(5), pp.92-97. Paul, P.A. and Munkvold, G.P., 2005. Regression and artificial neural network modeling for the prediction of gray leaf spot of maize. Phytopathology, 95(4), pp.388-396.

Pourreza, A., Lee, W. S., Ritenour, M. A., Roberts, P. 2016. Spectral Characteristics of Citrus Black Spot Disease. HortTechnology 26:254-260.

Rumpf, T.,Mahlein, A. K., Steiner, U., Oerke, E. C., Dehne, H. W., Pl¨umer, L. 2010. Early detection and classification of plant diseases with support vector machines based on hyperspectral reflectance. Comput. Electron. Agric. 74: 91-99.

Sanches, I.D.A., Souza Filho, C.R. and Kokaly, R.F., 2014. Spectroscopic remote sensing of plant stress at leaf and canopy levels using the chlorophyll 680 nm absorption feature with continuum removal. ISPRS Journal of Photogrammetry and Remote Sensing, 97, pp.111-122.

Shafri, H.Z. and Hamdan, N., 2009. Hyperspectral imagery for mapping disease infection in oil palm plantationusing vegetation indices and red edge techniques. American Journal of Applied Sciences, 6(6), p.1031.

Shafri, H.Z., Anuar, M.I., Seman, I.A., Noor, N.M., 2011. Spectral discrimination of healthy and Ganoderma-infected oil palms from hyperspectral data. International journal of remote sensing, 32(22), pp.7111-7129.

Smigaj, M., Gaulton, R., Barr, S.L., Suárez, J.C., 2015. UAV-borne thermal imaging for forest health monitoring: detection of disease-induced canopy temperature increase. ISPRS Int. Arch. Photogramm. Remote Sens. Spat. Inf. Sci, pp.349-354.

Tawfik, O., Shafri, H. M., Mohammed, A. A. 2013. Disease detection from field spectrometer data. IIUM Eng. J. 14:133-143.

Thenkabail, P. S., Enclona, E. A., Ashton, M. S., Van Der Meer, B. 2004. Accuracy assessments of hyperspectral waveband performance for vegetation analysis applications. Remote Sens. Environ. 91:354-376.

Trisakti, B., 2017, January. Vegetation type classification and vegetation cover percentage estimation in urban green zone using pleiades imagery. In IOP Conference Series: Earth and Environmental Science (Vol. 54, No. 1, p. 012003). IOP Publishing.

Wang, X., Zhang, M., Zhu, J., Geng, S., 2008. Spectral prediction of Phytophthora infestans infection on tomatoes using artificial neural network (ANN). International Journal of Remote Sensing, 29(6), pp.1693-1706.

West, J.S., Bravo, C., Oberti, R., Lemaire, D., Moshou, D., McCartney, H.A., 2003. The potential of optical canopy measurement for targeted control of field crop diseases. Annual review of Phytopathology, 41(1), pp.593-614.

Yang, Z., Rao, M. N., Elliott, N. C., Kindler, S. D., and Popham, T. W. 2009. Differentiating stress induced by greenbugs and Russian wheat aphids in wheat using remote sensing. Comput. Electron. Agric. 67:64-70.

Zamry, N.M., Zainal, A., Rassam, M.A., Bakhtiari, M., Maarof, M.A., 2015. Selection of Soil Features for Detection of Ganoderma Using Rough Set Theory. In Pattern Analysis, Intelligent Security and the Internet of Things (pp. 303-314). Springer, Cham.

Zhang, J., Pu, R., Huang, W., Yuan, L., Luo, J., Wang, J., 2012. Using in-situ hyperspectral data for detecting and discriminating yellow rust disease from nutrient stresses. Field Crops Research, 134, pp.165